



Published in final edited form as:

*J Magn Reson Imaging*. 2014 September ; 40(3): 609–615. doi:10.1002/jmri.24407.

## Comparison of retinal and cerebral blood flow between continuous arterial spin labeling MRI and fluorescent microsphere techniques

Yen-Yu I. Shih, PhD<sup>1,2</sup>, Bryan H. De La Garza, MS<sup>2</sup>, Shiliang Huang, PhD<sup>2</sup>, Guang Li, MS<sup>2</sup>, Lin Wang, PhD<sup>5</sup>, and Timothy Q. Duong, PhD<sup>2,3,4</sup>

<sup>1</sup>Departments of Neurology, Biomedical Research Imaging Center, and Biomedical Engineering, University of North Carolina, Chapel Hill, NC 27599, USA

<sup>2</sup>Research Imaging Institute, University of Texas Health Science Center at San Antonio, 8403 Floyd Curl Drive, San Antonio, TX 78229, USA

<sup>3</sup>Department of Ophthalmology, University of Texas Health Science Center at San Antonio, 8403 Floyd Curl Drive, San Antonio, TX 78229, USA

<sup>4</sup>Department of Radiology, University of Texas Health Science Center at San Antonio, 8403 Floyd Curl Drive, San Antonio, TX 78229, USA

<sup>5</sup>Devers Eye Institute, Legacy Clinical Research and Technology Center, 1225 NE 2nd Ave, Portland, OR 97208, USA

### Abstract

**Purpose**—To compare basal retinal and cerebral blood flow (BF) values using continuous arterial spin labeling (CASL) MRI and fluorescent microsphere.

**Materials and Methods**—A total of 41 animals were used. BF was measured using an established microsphere technique (a mixture of 2.5 million 8  $\mu$ m green and 0.5 million 10  $\mu$ m blue fluorescent microspheres) and CASL MRI blood flow measurement in the rat retina and brain at 7T and 11.7T, respectively.

**Results**—Retinal BF by MRI was  $1.18 \pm 0.57$  ml/g/min and choroidal BF was  $8.14 \pm 1.8$  ml/g/min ( $n=6$ ). Microsphere retinal BF was  $9.12 \pm 2.8$   $\mu$ l/min per tissue and choroidal BF was  $73.38 \pm 44$   $\mu$ l/min per tissue ( $n=18$ ), corresponding to a retinal BF value of  $1.22 \pm 0.36$  ml/g/min via a wet weight conversion. The wet-weight of the choroid could not be determined. To corroborate our findings, cerebral BF (CBF) by MRI was also analyzed. In the cerebral cortices, CBF was  $0.91 \pm 0.29$  ml/g/min ( $n=14$ ) by CASL MRI and  $1.09 \pm 0.37$  ml/g/min ( $n=6$ ) by microspheres. There were no significant differences found between MRI and microsphere blood flow in the retina and brain.

**Conclusion**—BF values in the rat retina and cerebral cortex by MRI are in agreement with those obtained by the microsphere technique.

### Keywords

MRI; microsphere; blood flow; retina; choroid; brain; rat

---

## INTRODUCTION

Arterial spin labeling (ASL) MRI is widely used to measure blood perfusion (refer as blood flow (BF) hereafter) because it is non-invasive, provides value in classical unit of milliliter per gram tissue per minutes, and can make repeated measurements every few seconds. Cerebral BF (CBF) MRI of the human brains has been compared with positron emission tomography (1). CBF of rodent brains has been compared with an invasive iodoantipyrine autoradiography (2).

High-resolution ASL MRI has recently been extended to image BF of the thin retina which measures ~250  $\mu\text{m}$  thick (including the choroid) in rodents. High-resolution continuous ASL (CASL) MRI can resolve the retinal and choroid BF layers in the rodent retinas (3,4). CASL MRI of the human retinas has also been reported (5,6). Retinal and choroid circulations exhibit differential responses to stimuli (7,8). MRI study of retinal and choroid blood flow has shown that they are perturbed in retinal degeneration (4,9), glaucoma (10) and diabetic retinopathy in animal models (11). There are no comparable non-invasive, depth-resolved methods to measure quantitative BF in the retina, and thus BF MRI could offer a unique means to study layer-specific perfusion of the normal and diseased retinas. High resolution BF MRI could provide invaluable information for preclinical and clinical studies of eye diseases.

The primary goal of this study was to compare retinal BF measurements in rats obtained by an established microsphere technique and by CASL. It has been recently demonstrated that the optimal size of the microspheres used in rats was 8  $\mu\text{m}$  for the retina; and 10  $\mu\text{m}$  for the choroid due to different capillary sizes between the two vascular beds (12,13). By using a mixture of the two different sized fluorescent microspheres with two different colors, the retina and choroid BF can be measured simultaneously in the same animal. CBF were also measured using microspheres and the CASL MRI techniques for further corroboration.

## MATERIALS AND METHODS

### Animal Preparation

All animal experiments were performed with IACUC approval. Adult male Sprague Dawley rats (n=41, 250–300 g) were initially anesthetized with 2% isoflurane, intubated, and ventilated, similar to that described previously (8,13,14). End-tidal  $\text{CO}_2$ , body temperature, oxygen saturation, and heart rate were continuously monitored and kept within normal range (3–3.5%, 37°C, ~98%, and ~400 beats/min, respectively). The right femoral artery and vein were cannulated for arterial blood pressure (MABP)/blood gas measurements and drug administration, respectively. After the surgery, the isoflurane level was reduced to 1.2–1.5%

and the animal was then placed on a custom-built head holder. MABP was continuously monitored and maintained between 90–110 mmHg using hetastarch (0.5–1.5 ml/animal, i.v.). Atropine eye drop was applied topically to dilate the pupil and a muscle relaxant, pancuronium bromide (3 mg/kg, i.v.) was administered. Arterial carbon dioxide partial pressure (PaCO<sub>2</sub>) was measured and maintained at 35–40 mmHg by adjusting tidal volume. The eyes were dark adapted for at least 30 min before BF measurement. All the subjects were dark adapted for at least 30 min before BF measurement.

### MRI Blood Flow Measurement

MRI retinal and choroidal BF measurements (n=6) were performed by an 11.7 T/16 cm magnet and a 74 G/cm B-GA9S gradient insert (Bruker, Billerica, MA). A custom-made small circular transceiver surface coil (ID~7 mm) was placed on the left eye. The diameter of the coil was previously optimized to achieve the best SNR at the appropriate depth (4,7,15–17). Quantitative BF MRI was acquired using CASL technique with 6-shot, gradient echo EPI, spectral width=208 kHz, TR/TE=3000/12.7 ms, labeling duration=2.96 s, FOV=10×10 mm, slice thickness=0.6 mm, and acquisition matrix=228×228. The retina image was linearized by radially projecting lines perpendicular to the retinal surface. Care was taken to minimize data misregistration. Scout images were first acquired to plan a single mid-sagittal slice bisecting the center of the eye and optic nerve for subsequent imaging. Moreover, by choosing a single center slice, partial-volume effect due to the retinal curvature due to thick imaging slice could also be minimized (7,15,16). Basal BF profiles were then averaged along the length of the retina (4). BF was calculated as (18):

$$BF = \frac{\lambda}{T_1} \frac{S_C - S_L}{S_L + (2\alpha - 1)S_C}$$

where  $S_C$  and  $S_L$  are the MR signal intensities from the control and labeled images, respectively.  $\lambda$ , the tissue–blood partition coefficient of water, was taken to be 0.9, the same as in the brain (19).  $\lambda$ , a difficult measurement, has not been reported for the retina or choroid. The labeling efficiency  $\alpha$  was previously measured to be 0.7 in the distal internal carotid arteries at the base of the frontal lobe (4,20). The retina and choroid T1 at 11.7T was taken to be 2.1 s (21).

CBF was measured at a 7 T/30 cm magnet and a 40 G/cm gradient (Bruker, Billerica, MA) (n=14) with single-shot, gradient echo EPI, spectral width=200 kHz, TR/TE=3000/10.3 ms, labeling duration=2.46 s, post-labeling delay=0.25 s, FOV=25.6×25.6 mm, slice thickness=1.5 mm, and acquisition matrix=96×96. CBF values were calculated similarly as the retinal and choroidal BF, except T<sub>1</sub>=1.8 s was used.

### Microsphere Blood Flow Measurement

In a separate group of rats (n=18), the retinal and choroidal BF was measured using a modified microsphere technique (12). Microsphere and CASL blood flow measurements were not performed on the same time on the same subject due to technical constraint. A mixture of 2.5 million 8 μm green and 0.5 million 10 μm blue fluorescent microspheres (FluoSpheres, Molecular Probes, Eugene, OR) were used. The microspheres were suspended within approximately 350 to 550 μl solution of 0.15 M NaCl and 0.05% Tween 20. The suspension was stored in a 37°C water bath and sonicated for 10–20 s immediately before injection. The dose and the size of the microspheres for ocular BF measurement in rats have

been optimized (12,13) by evaluating microspheres of different diameters (6, 8, 10, or 15  $\mu\text{m}$ ) and concentrations ( $10^6$ ,  $5 \times 10^6$ , or  $10^7$  microspheres). The results showed that 8  $\mu\text{m}$ ,  $5 \times 10^6$  microspheres resulted in a highest entrapped number and a homogenous distribution in the retina, while 10  $\mu\text{m}$ ,  $10^6$  microspheres was optimal for the choroid. These findings were adapted to the present study.

A 2-cm vertical incision was made along the midline of the abdomen below the xiphoid. The incision was kept open using an ocular speculum to allow the apex of the heart to be visualized through the diaphragm. Heparin (0.5–1 mg/kg, I.V.) was administered to prevent blood clotting. A 27-gauge needle, connected to 15-cm PE50 tubing, was inserted into the left ventricle through the diaphragm. A mixture of dual size microspheres was then injected into the left ventricle. The injection duration was 35–40 s. Arterial blood sample was passively collected for one minute at a rate of  $\sim 0.5$  ml/min after the onset of microsphere injection.

The eyes were then enucleated and the anterior portion of the eye, approximately 2 mm behind the limbus, was removed (including cornea, iris, lens, and ciliary body). The entire retina was dissected from the remaining eyecup and flat-mounted on a glass slide. The choroid together with the underlying sclera was also flat-mounted with four tension-relief cuts. The tissues were sealed with fluorescence mounting medium (Vectashield, Vector Laboratories, Burlingame, CA) and cover slips. The number of microspheres was counted in the retina (8  $\mu\text{m}$ ) and the choroid (10  $\mu\text{m}$ ) under a fluorescent microscope with an image analysis system (Bioquant, R&M Biometrics, Inc. Nashville, TN). The number of microspheres of each color in the arterial reference blood samples was also counted after the blood was haemolyzed, diluted and applied to a hemocytometer counting chamber (Hausser Scientific, Horsham, PA). The concentration of each colored/fluorescent microspheres in the reference blood samples was determined. The BF in each retina and choroid was calculated by the following equation:

$$\text{Blood flow per tissue } (\mu\text{l/min}) = \frac{\text{number of microspheres per tissue}}{\text{number of microspheres in reference blood}} \times \text{reference blood flow } (\mu\text{l/min})$$

BF in  $\mu\text{l/min}$  was converted to ml/g/min using an averaged retina wet weight of 7.5 mg (22,23).

In a sub-group of rats (n=6), the brains were freshly removed at the end of the microsphere experiments and preserved in 5% formalin. To minimize ice crystals from forming during rapid freezing process, brain tissue was transferred to 20% sucrose in phosphate buffered saline (PBS), and then transferred to 30% sucrose in PBS. Brain tissue was allowed to be fully impregnated with sucrose in each step before rapid freezing. Brains were then frozen in nitrogen cooled isopentane and sliced at 20 $\mu$  with cryostat. Two adjacent 20  $\mu\text{m}$  slices were collected for 3 slice locations corresponding to MRI data. Locations of slices were selected using rat brain atlas as a reference. Brain slices were sealed with fluorescence mounting medium (Vectashield, Vector Laboratories, Burlingame, CA) and cover slipped. Whole brain microsphere images for each brain were achieved by taking individual fluorescent microscope images at 4x magnification in a serpentine direction and stitched together using

Microsoft image composite editor. Microspheres were counted using imageJ software, using rat brain atlas to define regions of interest.

BF was converted to ml/g/min using a brain wet weight of  $1.993 \pm 0.11$  g and brain volume of  $1.849 \pm 0.06$  ml measured from three animals with matched age and body weight, resulting a tissue density of  $0.0011$  g/mm<sup>3</sup>. This density was assumed to be the same in different brain areas. The volume of each brain regions was defined according to the ROIs on the atlas in a unit of mm<sup>2</sup> multiplying the slice thickness (0.04 mm).

Statistical analysis for retinal and choroidal BF comparisons was performed by paired t-tests. Multiple comparisons for CBF were performed by ANOVA with Bonferroni posthoc test. A probability value of  $p < 0.05$  was set as the level for rejecting the null hypothesis. All data in text are expressed as mean  $\pm$  SD. Of note, an earlier study showed that microsphere technique is able to detect up to 80% increases in retinal BF under hypercapnic challenge (from PaCO<sub>2</sub> of 35 mmHg to 45 mmHg) while the choroid BF was not affected (25). A statistic power calculation based on the pilot data showed that at a probability of 5% and a power of 80% with unpaired t-test, it requires 12 and 18 animals to demonstrate a potential 25% difference in retinal and choroidal BF between two groups, respectively (13).

## RESULTS

All animals were non-invasively monitored for EtCO<sub>2</sub>, oxygen saturation, heart rate, and rectal temperature and these parameters were within normal physiological ranges. In 18 rats, invasive arterial pCO<sub>2</sub>, pH, and MABP were also measured and these parameters were  $38.5 \pm 3.5$  mmHg,  $7.46 \pm 0.04$ , and  $101 \pm 12$  mmHg, respectively.

Figure 1a shows basal ocular BF map at  $44 \times 44$   $\mu$ m in plane resolution by MRI. The averaged BF values in the retina and the choroid were  $1.18 \pm 0.57$  and  $8.14 \pm 1.8$  ml/g/min, respectively (n=6). The retina and the choroid BF values were significantly different from each other ( $p=0.00008$ ). The ratio of MRI retinal to choroidal BF was 1:6.9.

Figure 1b show representative fluorescent images of the retina and choroid. Green (8  $\mu$ m) microspheres were counted in the retina and blue (10  $\mu$ m) microspheres were counted in the choroid. The retinal and choroidal BF values were  $9.12 \pm 2.8$  and  $73.38 \pm 44$   $\mu$ l/min per tissue, respectively (n=18). The retina and the choroid BF values were significantly different from each other ( $p=0.0008$ ). The ratio of microsphere retinal to choroidal BF was 1:10.8. Using the average wet weight of the rat retina reported previously (7.5 mg) (22,23), the retinal BF by microspheres was  $1.22 \pm 0.36$  ml/g/min (n=18), which is not significantly different from retinal BF measured by MRI ( $p=0.85$ ). The power of our statistical test was 5.2%. Even if the sample size of the MRI study was increased to  $n = 18$  to make a sample size ratio of 1:1, the power would only increase to 5.7%. On the other hand, to reject our null hypothesis of no difference, with a sample size ratio of 1:1, we need a sample size of  $n = 2230$  for each group to detect a difference of 0.04 ml/g/min (i.e. only ~3% of mean retinal BF). Even if this ~3% difference is proved to be statistically significant, it is not physiologically important. Hence, a larger sample size would not change our conclusion of retinal BF comparison. The choroidal BF is difficult to be converted into ml/g/min unit because the choroid is a vascular

structure and its wet weight is unknown. The choroid-retinal pigment epithelium was assumed to be 0.0225 g according to the data published previously (24). By adapting this number, the choroid BF was  $3.26 \pm 1.95$  ml/g/min. Note that the choroidal BF may be more significantly underestimated because the majority of the weight was from retinal pigment epithelium instead of choroid.

CBF maps at  $200 \times 200$   $\mu\text{m}$  in plane resolution by MRI are shown in Figure 2a. Total microsphere distributions ( $n=6$ ) in the brain are shown in Figure 2b. The ROIs used for CBF analysis are shown in Figure 2c. Group-averaged CBF values by MRI and microsphere are compared in Figure 2d. CBF in the cerebral cortex was  $0.91 \pm 0.29$  ml/g/min by MRI and was not significantly different from that of the 10  $\mu\text{m}$  ( $1.09 \pm 0.37$  ml/g/min,  $p=0.99$ ) and the 8  $\mu\text{m}$  ( $1.38 \pm 0.44$  ml/g/min,  $p=0.09$ ) microsphere data. CBF in the striatum by MRI was not significantly different from that of the 10  $\mu\text{m}$  microsphere data ( $p=0.55$ ), but significantly lower than 8  $\mu\text{m}$  microsphere data ( $p=0.001$ ).

Blood flow values for individual animals from different regions are listed in Table 1.

## DISCUSSION

MRI retinal and choroidal BFs in this study were 1.18 and 8.14 ml/g/min, respectively, with a ratio of 1:6.9 (Sprague Dawley rats). These values are in good agreement with recent reports measuring ocular BF in pigmented Long Evans rats of 0.97 and 7.70 ml/g/min (ratio=1:6) (4), and C57BL/6 mice of 1.3 and 7.7 ml/g/min (ratio 1:8) (3), respectively, under isoflurane and similar experimental conditions.

For the microsphere BF measurement, Wang and colleagues recently modified the traditional microsphere method by comparing various microspheres size and doses to enable reliable retinal and choroidal BF measurements for rats (12). It has been shown that microspheres smaller than the most commonly used size, 15  $\mu\text{m}$ , are required to reliably measure rat ocular BF. The optimal dose and size of the microspheres used in rats was 2.5 million and 8  $\mu\text{m}$  diameter for the retina; and 0.5 million and 10  $\mu\text{m}$  diameter for the choroid due to different capillary sizes between the two vascular beds. By using a mixture of the two different sized fluorescent microspheres with two different colors, the retina and choroidal BF can be measured in the same animals. This modified microsphere technique has been used to detect retinal and choroidal BF changes induced by hypocapnia and hypercapnia in rats (25). We used this technique and showed that the basal retinal and choroidal BFs were 9 and 73  $\mu\text{l}/\text{min}$ , respectively, in Sprague Dawley rats. Compared to the published literature, both the retinal and the choroidal BF were lower than Brown-Norway rats ( $\sim 15$  and 166  $\mu\text{l}/\text{min}$ , respectively) (25). This could be attributed to the species difference. The Sprague Dawley rats, unlike the Brown-Norway rats, do not have retinal pigment epithelium and do not develop neovascularization in the retina after injury (26). In addition, functions of their retinal cone cells are also different as shown by photopic and scotopic flicker electroretinograms (27).

Microsphere data express BF in unit of  $\mu\text{l}/\text{min}$ . Converting from  $\mu\text{l}/\text{min}$  to ml/g/min requires wet weight value which is difficult to determine. In dissecting the retina, some vitreous

humor is attached to the retina and it cannot be easily removed from the retina without affecting the microspheres in the retinal vessels. The choroid is essentially a vascular structure and is only about 100  $\mu\text{m}$  thick *in vivo*. Its wet weight is very difficult to obtain because the vessels collapse and could not be readily separated from the retinal pigment epithelium and sclera. By adapting the wet weight of the rat retina in the published literature (22,23), the microsphere retinal BF in the present study was 1.22 ml/g/min, which is comparable to the MRI retinal BF (1.18 ml/g/min).

Our CASL MRI CBF values are similar to previous reports (2,28–31). Cortical CBF has been reported to be 0.74 ml/g/min by  $\text{H}_2^{17}\text{O}$  MRI (32), 0.91 ml/g/min by flow-sensitive alternating inversion recovery (FAIR) MRI (2) and 0.85 ml/g/min by iodoantipyrine autoradiography (2). Hernandez et al. previously compared CBF by MRI and microsphere in a conference abstract (33). CBF was measured using ASL with a single quadrature bird-cage coil and a line-scan technique for a single slice with  $3\times 3$  mm resolution. Six voxels in the brain per subject were sampled to calculate CBF. High correlation was found in that study. By contrast, our multislice CBF images had  $0.26\times 0.26$  mm resolution, ROI was defined according to the brain atlas with clear anatomical outline, and the microspheres were counted for the corresponding MRI brain sections under a fluorescent microscope. Our data showed that CBF of the rat cortex was 0.91 ml/g/min by MRI and 1.09 or 1.38 ml/g/min by microspheres, in reasonable agreement with the above-mentioned previous reports. Striatal CBF by MRI and 10  $\mu\text{m}$  microspheres were also similar. This consistency leads credibility to retinal and choroidal BF data as microsphere data of the retina and brain were obtained in the same animals. Additionally, perfusion can also be measured by contrast agent technique. MRI-derived cerebral (34) and myocardial (35,36) BF using exogenous contrast agent has been previously validated using microspheres. Excellent correlation in blood flow was reported between two techniques.

In the MRI and PET literatures, subcortical CBF is overall smaller or similar to cortical CBF (2,28–31,37), as we observed in our study. Our microsphere data showed that striatal CBF by 8  $\mu\text{m}$  microspheres was higher than that by MRI. In addition, MRI CBF also showed better tissue heterogeneity than microsphere CBF. The distribution of microspheres did not quite resemble the MRI CBF because it has been shown that more of the larger microspheres were trapped at peripheral pre-capillary arterioles, resulting in higher counts in tissue with smaller vessel size. In contrast, more of the smaller microspheres are trapped in tissue with higher vascular density. A typical example is that 8  $\mu\text{m}$  microsphere showed highest counts at the center of the retina but the lowest counts at the edge of the retina, whereas the distribution of 15  $\mu\text{m}$  microsphere was completely opposite, showing lowest counts at the center and highest counts at the edge (12). These findings indicate that single size microsphere may not be suitable to describe flow distribution in an organ with high heterogeneity.

The present quantitative study evaluated the sub-regional CBF using fluorescent microspheres. The microsphere size and dose in the rat brain, unlike that in the retina and choroid, has not been previously optimized and warrants further elucidation for more accurate CBF quantitation. Only a few studies attempted to use fluorescent microspheres to measure CBF in rats (38) and microsphere size other than 15  $\mu\text{m}$  has not been tested. The 15

$\mu\text{m}$  microsphere was not used in this study because our previous data showed that microsphere at 15  $\mu\text{m}$  tended to lodge in pre-capillary arterioles and caused significant MABP increase (up to 30 mmHg) during the injection, where 8 and 10  $\mu\text{m}$  microspheres did not significantly alter MABP. Our data suggest that microsphere with a size of 8 or 10  $\mu\text{m}$  can be useful for cortical CBF measurement, but 8  $\mu\text{m}$  microspheres may not be suitable to measure subcortical CBF due to difference in vessel size and density. Both 8 and 10  $\mu\text{m}$  microspheres did not resemble MRI CBF heterogeneity. Caution has to be taken when assessing multi-regional CBF with single size microsphere.

In conclusion, the present study demonstrated that basal BF values measured by MRI are in agreement with the microsphere technique in the rat retina.

## Acknowledgments

**Grant support:** This work was supported in part by the NIH/NEI (R01 EY014211 and EY018855), MERIT Award from the Department of Veterans Affairs, and San Antonio Life Science Institute to TQD, and American Heart Association (10POST4290091), Clinical Translational Science Award (CTSA, parent grant UL1RR025767), and San Antonio Area Foundation to YYIS.

## References

- Chen JJ, Wieckowska M, Meyer E, Pike GB. Cerebral blood flow measurement using fMRI and PET: a cross-validation study. *International journal of biomedical imaging*. 2008; 2008:516359. [PubMed: 18825270]
- Tsekos NV, Zhang F, Merkle H, Nagayama M, Iadecola C, Kim SG. Quantitative measurements of cerebral blood flow in rats using the FAIR technique: correlation with previous iodoantipyrine autoradiographic studies. *Magn Reson Med*. 1998; 39(4):564–573. [PubMed: 9543418]
- Muir ER, Duong TQ. MRI of retinal and choroidal blood flow with laminar resolution. *NMR in biomedicine*. 2011; 24(2):216–223. [PubMed: 20821409]
- Li G, De La Garza B, Shih YY, Muir ER, Duong TQ. Layer-specific blood-flow MRI of retinitis pigmentosa in RCS rats. *Exp Eye Res*. 2012; 101:90–96. [PubMed: 22721720]
- Peng Q, Zhang Y, Nateras OS, van Osch MJ, Duong TQ. MRI of blood flow of the human retina. *Magn Reson Med*. 2011; 65(6):1768–1775. [PubMed: 21590806]
- Maleki N, Dai W, Alsop DC. Blood flow quantification of the human retina with MRI. *NMR in biomedicine*. 2011; 24(1):104–111. [PubMed: 20862658]
- Shih YY, De la Garza BH, Muir ER, Rogers WE, Harrison JM, Kiel JW, Duong TQ. Lamina-specific functional MRI of retinal and choroidal responses to visual stimuli. *Invest Ophthalmol Vis Sci*. 2011; 52(8):5303–5310. [PubMed: 21447679]
- Shih YY, Muir ER, Li G, De La Garza BH, Duong TQ. High-Resolution 3D MR Microangiography of the Rat Ocular Circulation. *Radiology*. 2012; 264(1):234–241. [PubMed: 22523323]
- Muir ER, De La Garza B, Duong TQ. Blood flow and anatomical MRI in a mouse model of retinitis pigmentosa. *Magn Reson Med*. 2013; 69(1):221–228. [PubMed: 22392583]
- Lavery WJ, Muir ER, Kiel JW, Duong TQ. Magnetic resonance imaging indicates decreased choroidal and retinal blood flow in the DBA/2J mouse model of glaucoma. *Invest Ophthalmol Vis Sci*. 2012; 53(2):560–564. [PubMed: 22205612]
- Muir ER, Renteria RC, Duong TQ. Reduced ocular blood flow as an early indicator of diabetic retinopathy in a mouse model of diabetes. *Invest Ophthalmol Vis Sci*. 2012; 53(10):6488–6494. [PubMed: 22915034]
- Wang L, Fortune B, Cull G, McElwain KM, Cioffi GA. Microspheres method for ocular blood flow measurement in rats: size and dose optimization. *Exp Eye Res*. 2007; 84(1):108–117. [PubMed: 17069799]



13. Shih YY, Wang L, De La Garza BH, Li G, Cull G, Kiel JW, Duong TQ. Quantitative retinal and choroidal blood flow during light, dark adaptation and flicker light stimulation in rats using fluorescent microspheres. *Curr Eye Res.* 2013; 38(2):292–298. [PubMed: 23317112]
14. Shih YY, Li G, Muir ER, De La Garza BH, Kiel JW, Duong TQ. Pharmacological MRI of the choroid and retina: Blood flow and BOLD responses during nitroprusside infusion. *Magn Reson Med.* 2012; 68(4):1273–1278. [PubMed: 22183830]
15. Cheng H, Nair G, Walker TA, Kim MK, Pardue MT, Thule PM, Olson DE, Duong TQ. Structural and functional MRI reveals multiple retinal layers. *Proc Natl Acad Sci USA.* 2006; 103:17525–17530. [PubMed: 17088544]
16. Shih YY, Li G, Muir ER, De La Garza BH, Kiel JW, Duong TQ. Pharmacological MRI of the choroid and retina: Blood flow and BOLD responses during nitroprusside infusion. *Magn Reson Med.* 2011
17. Li G, Shih YY, Kiel JW, De La Garza BH, Du F, Duong TQ. MRI study of cerebral, retinal and choroidal blood flow responses to acute hypertension. *Exp Eye Res.* 2013; 112:118–124. [PubMed: 23623996]
18. Zhang W, Silva AC, Williams DS, Koretsky AP. NMR measurement of perfusion using arterial spin labeling without saturation of macromolecular spins. *Magn Reson Med.* 1995; 33(3):370–376. [PubMed: 7760704]
19. Herscovitch P, Raichle ME. What is the correct value for the brain--blood partition coefficient for water? *J Cereb Blood Flow Metab.* 1985; 5(1):65–69. [PubMed: 3871783]
20. Muir ER, Shen Q, Duong TQ. Cerebral blood flow MRI in mice using the cardiac-spin-labeling technique. *Magn Reson Med.* 2008; 60(3):744–748. [PubMed: 18727091]
21. Chen J, Wang Q, Zhang H, Yang X, Wang J, Berkowitz BA, Wickline SA, Song SK. In vivo quantification of T1, T2, and apparent diffusion coefficient in the mouse retina at 11. 74T. *Magn Reson Med.* 2008; 59(4):731–738. [PubMed: 18383302]
22. Tilton RG, Chang KC, LeJeune WS, Stephan CC, Brock TA, Williamson JR. Role for nitric oxide in the hyperpermeability and hemodynamic changes induced by intravenous VEGF. *Invest Ophthalmol Vis Sci.* 1999; 40(3):689–696. [PubMed: 10067972]
23. Winkler BS, Arnold MJ, Brassell MA, Sliter DR. Glucose dependence of glycolysis, hexose monophosphate shunt activity, energy status, and the polyol pathway in retinas isolated from normal (nondiabetic) rats. *Invest Ophthalmol Vis Sci.* 1997; 38(1):62–71. [PubMed: 9008631]
24. Kadam RS, Kompella UB. Influence of lipophilicity on drug partitioning into sclera, choroid-retinal pigment epithelium, retina, trabecular meshwork, and optic nerve. *The Journal of pharmacology and experimental therapeutics.* 2010; 332(3):1107–1120. [PubMed: 19926800]
25. Wang L, Grant C, Fortune B, Cioffi GA. Retinal and choroidal vasoreactivity to altered PaCO<sub>2</sub> in rat measured with a modified microsphere technique. *Exp Eye Res.* 2008; 86(6):908–913. [PubMed: 18420196]
26. Gao G, Li Y, Fant J, Crosson CE, Becerra SP, Ma JX. Difference in ischemic regulation of vascular endothelial growth factor and pigment epithelium--derived factor in brown norway and sprague dawley rats contributing to different susceptibilities to retinal neovascularization. *Diabetes.* 2002; 51(4):1218–1225. [PubMed: 11916948]
27. Rosolen SG, Chalier C, Rigaudiere F, Lachapelle PL, GJ, Flicker ERG. Evidence that Sprague Dawley and Brown Norway Rats Have Different Cone-mediated Responses. *Invest Ophthalmol Vis Sci.* 2003; 44:1903–B1799.
28. Danker JF, Duong TQ. Quantitative regional cerebral blood flow MRI of animal model of attention-deficit/hyperactivity disorder. *Brain research.* 2007; 1150:217–224. [PubMed: 17391651]
29. Shen Q, Duong TQ. Background suppression in arterial spin labeling MRI with a separate neck labeling coil. *NMR in biomedicine.* 2011; 24(9):1111–1118. [PubMed: 21294207]
30. Silva AC, Kim SG, Garwood M. Imaging blood flow in brain tumors using arterial spin labeling. *Magn Reson Med.* 2000; 44(2):169–173. [PubMed: 10918313]
31. Meng Y, Wang P, Kim SG. Simultaneous measurement of cerebral blood flow and transit time with turbo dynamic arterial spin labeling (Turbo-DASL): application to functional studies. *Magn Reson Med.* 2012; 68(3):762–771. [PubMed: 22162211]

32. Zhu XH, Merkle H, Kwag JH, Ugurbil K, Chen W. 17O relaxation time and NMR sensitivity of cerebral water and their field dependence. *Magn Reson Med.* 2001; 45(4):543–549. [PubMed: 11283979]
33. Hernandez L, Branch CA, Helpert JA. Measurement of CBF with Arterial Spin Labeling: Correlate with Microspheres. *Proc Intl Soc Mag Reson Med.* 1998
34. Goetze AHG, Bock JC, Heyer C, Weinmann HJ, Felix R. Experimental validation of susceptibility-contrast cerebral blood flow measurement by a microsphere reference method. *Proc Soc Mag Reson.* 1994
35. Miller DD, Holmvang G, Gill JB, Dragotakes D, Kantor HL, Okada RD, Brady TJ. MRI detection of myocardial perfusion changes by gadolinium-DTPA infusion during dipyridamole hyperemia. *Magn Reson Med.* 1989; 10(2):246–255. [PubMed: 2761383]
36. Wilke N, Simm C, Zhang J, Ellermann J, Ya X, Merkle H, Path G, Ludemann H, Bache RJ, Ugurbil K. Contrast-enhanced first pass myocardial perfusion imaging: correlation between myocardial blood flow in dogs at rest and during hyperemia. *Magn Reson Med.* 1993; 29(4):485–497. [PubMed: 8464365]
37. Yee SH, Jerabek PA, Fox PT. Non-invasive quantification of cerebral blood flow for rats by microPET imaging of 15O labelled water: the application of a cardiac time-activity curve for the tracer arterial input function. *Nucl Med Commun.* 2005; 26(10):903–911. [PubMed: 16160650]
38. De Visscher G, Haseldonckx M, Flameng W. Fluorescent microsphere technique to measure cerebral blood flow in the rat. *Nat Protoc.* 2006; 1(4):2162–2170. [PubMed: 17487208]

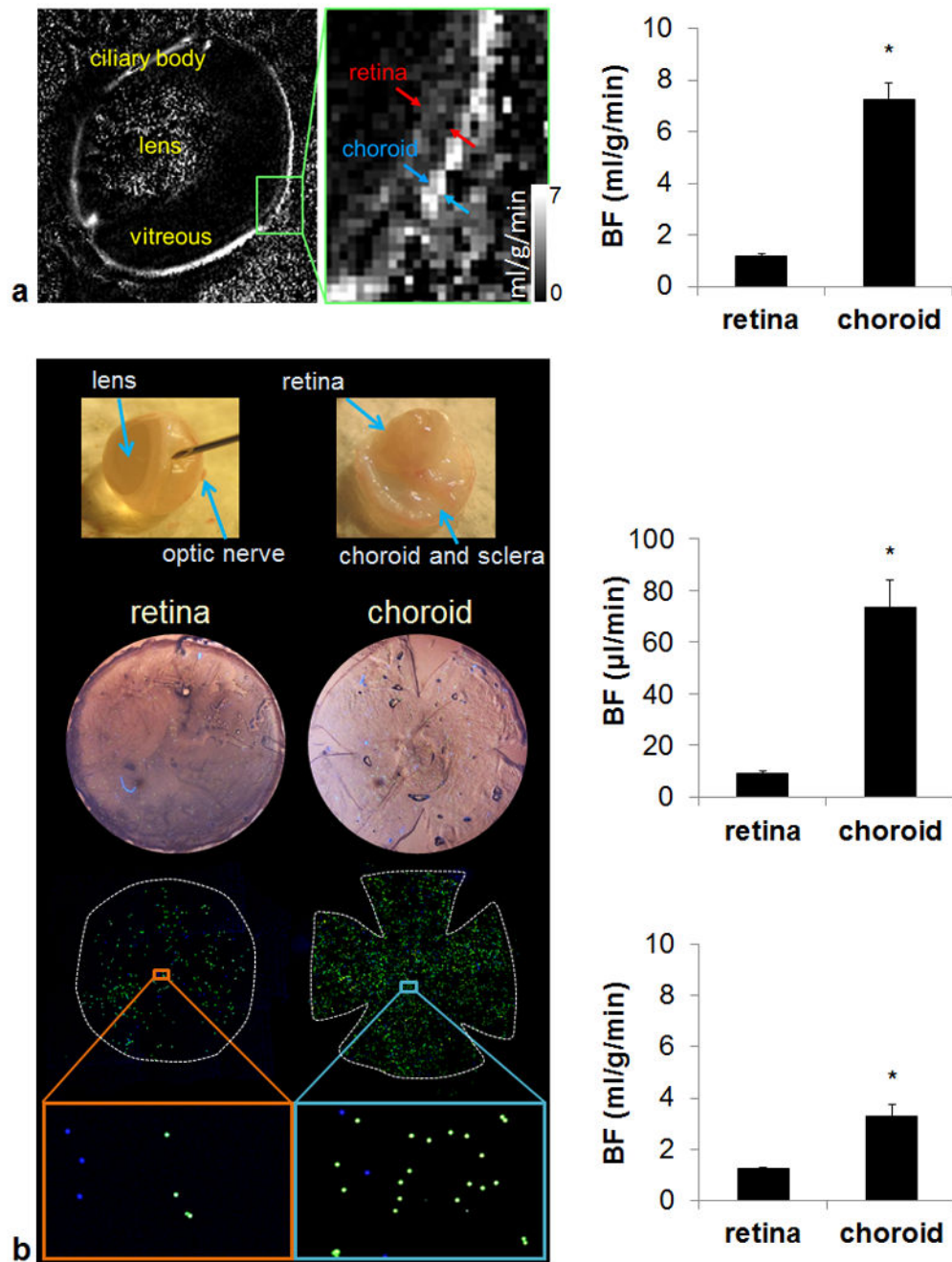


**Figure 1.** Quantitative basal retinal and choroidal blood flow measurement by high-resolution MRI and fluorescent microspheres. **(a)** A representative ocular blood flow map and group-averaged blood flow values ( $n = 6$ ). Images were acquired at  $44 \times 44 \mu\text{m}$  resolution and scaled from 0 – 7 ml/g/min. **(b)** Flat-mount process and representative fluorescent microsphere images of the retina and choroid and group-averaged blood flow values by microsphere ( $n = 18$ ). \* $p < 0.05$ . Error bars are S.E.M.

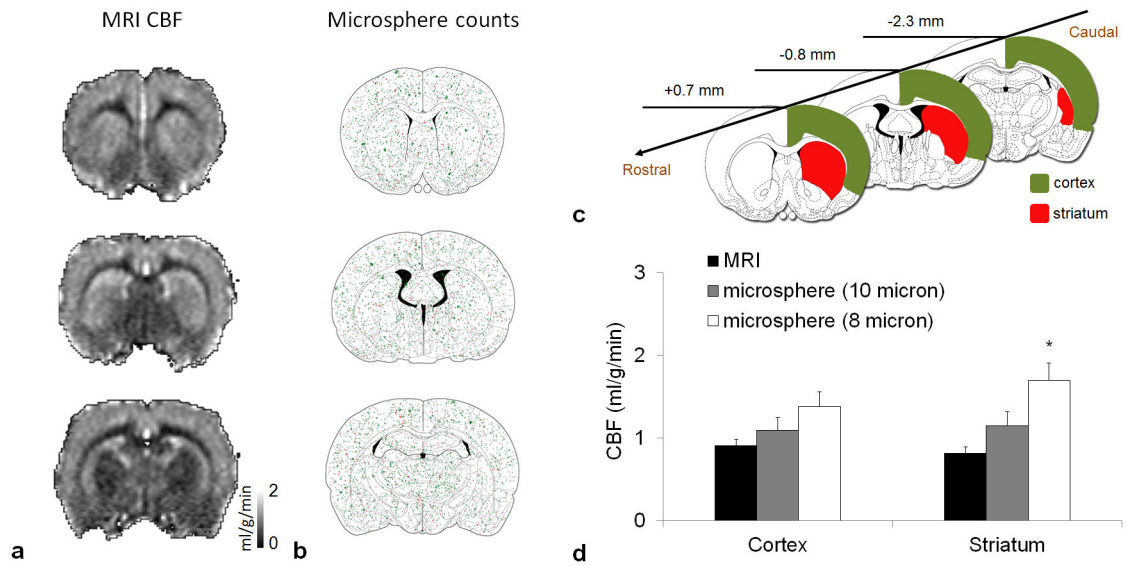


**Figure 2.**

Quantitative basal cerebral blood flow measurement by high-resolution MRI and fluorescent microspheres. **(a)** A representative cerebral blood flow map acquired at  $200 \times 200 \mu\text{m}$  resolution. Images were scaled from 0 – 2 ml/g/min. **(b)** Distribution of total fluorescent microspheres ( $n = 6$ ). Green dots represent  $8 \mu\text{m}$  and red dots represent  $10 \mu\text{m}$  microspheres. **(c)** Region of interest on the brain atlas. **(d)** Quantitative cerebral blood flow measured by MRI ( $n = 14$ ) and microsphere ( $n = 6$ ). \* $p < 0.05$ , significantly different from MRI data. Error bars are S.E.M.

**Table 1**

Microsphere and MRI blood flow values of all measured subjects.

Subject	Microsphere blood flow measurement						MRI blood flow measurement									
	Retina		Choroid		Cortex		Striatum		Retina		Choroid		Cortex		Striatum	
	$\mu\text{l}/\text{min}$	$\text{ml}/\text{g}/\text{min}$	$\mu\text{l}/\text{min}$	$\text{ml}/\text{min}$	$\text{ml}/\text{g}/\text{min}$	$\text{ml}/\text{g}/\text{min}$ (8 $\mu$ spheres)	$\text{ml}/\text{g}/\text{min}$ (10 $\mu$ spheres)	$\text{ml}/\text{g}/\text{min}$ (8 $\mu$ spheres)	$\text{ml}/\text{g}/\text{min}$ (10 $\mu$ spheres)	$\text{ml}/\text{g}/\text{min}$ (10 $\mu$ spheres)	$\text{ml}/\text{g}/\text{min}$	$\text{ml}/\text{g}/\text{min}$	$\text{ml}/\text{g}/\text{min}$	$\text{ml}/\text{g}/\text{min}$	$\text{ml}/\text{g}/\text{min}$	$\text{ml}/\text{g}/\text{min}$
1	7.86	1.05	55.80	2.48	0.70	0.84	0.97	1.43	1.08	8.99	0.83	0.77				
2	12.50	1.67	98.33	4.37	1.47	1.62	1.30	2.36	1.92	9.84	1.18	1.17				
3	10.09	1.35	40.19	1.79	1.07	1.81	0.78	1.71	1.00	8.63	0.87	0.78				
4	8.65	1.16	64.59	2.87	1.03	1.48	1.45	2.03	1.75	9.41	1.39	1.18				
5	7.20	0.96	69.80	3.10	1.58	1.71	1.76	1.82	0.36	6.80	0.98	0.81				
6	4.96	0.67	43.22	1.92	0.72	0.83	0.62	0.86	0.97	5.16	0.83	0.62				
7	8.39	1.12	114.73	5.10							0.59	0.54				
8	5.57	0.75	31.62	1.40							0.56	0.59				
9	6.09	0.81	52.54	2.34							0.87	0.85				
10	7.52	1.00	37.51	1.67							1.38	1.33				
11	9.10	1.21	40.42	1.80							0.81	0.76				
12	15.57	2.08	53.31	2.37							1.27	1.13				
13	10.89	1.45	21.20	0.94							0.64	0.53				
14	11.10	1.48	87.31	3.88							0.50	0.40				
15	9.00	1.20	40.52	1.80												
16	13.71	1.83	163.16	7.25												
17	8.53	1.13	140.52	6.25												
18	7.43	0.99	166.10	7.38												
mean	9.12	1.22	73.38	3.26	1.09	1.38	1.15	1.70	1.18	8.14	0.91	0.82				
SD	2.8	0.36	44.00	1.95	0.37	0.44	0.43	0.52	0.57	1.80	0.29	0.28				